Insights from Crystallographic Studies into the Structural and Pairing Properties of Nucleic Acid Analogs and Chemically Modified DNA and RNA Oligonucleotides

Martin Egli and Pradeep S. Pallan

Department of Biochemistry, School of Medicine, Vanderbilt University, Nashville, Tennessee 37232; email: martin.egli@vanderbilt.edu

Annu. Rev. Biophys. Biomol. Struct. 2007. 36:281–305

The *Annual Review of Biophysics and Biomolecular Structure* is online at biophys.annualreviews.org

This article's doi: 10.1146/annurev.biophys.36.040306.132556

1056-8700/07/0609-0281$20.00

Key Words

antisense, hydration, nuclease resistance, nucleic acid etiology, RNA affinity, RNA interference

Abstract

Chemically modified nucleic acids function as model systems for native DNA and RNA; as chemical probes in diagnostics or the analysis of protein–nucleic acid interactions and in high-throughput genomics and drug target validation; as potential antigene-, antisense-, or RNAi-based drugs; and as tools for structure determination (i.e., crystallographic phasing), just to name a few. Biophysical and structural investigations of chemically modified DNAs and RNAs, particularly of nucleic acid analogs with more significant alterations to the well-known base-sugar-phosphate framework (i.e., peptide or hexopyranose nucleic acids), can also provide insights into the properties of the natural nucleic acids that are beyond the reach of studies focusing on DNA or RNA alone. In this review we summarize results from crystallographic analyses of chemically modified DNAs and RNAs that are primarily of interest in the context of the discovery and development of oligonucleotide-based therapeutics. In addition, we re-examine recent structural data on nucleic acid analogs that are investigated as part of a systematic effort to rationalize nature's choice of pentose in the genetic system.

Contents

INTRODUCTION 282
SUGAR MODIFICATIONS 284
- Ribose 2′-O Modifications 284
- 2′-Amine-Substituted RNA 287
- Arabinonucleic Acid and 2′-Deoxy-2′-Fluoroarabinonucleic Acid 287
- 4′-Thio-RNA 288

BASE MODIFICATIONS 289
- Base Analogs with Cationic Tethers 289
- *Cis-syn* Thymine Dimer 290
- DNA Conjugates with Stilbene-Diether Linkers 290
- Difluorotoluene Analog of T 291

NUCLEIC ACID ANALOGS 292
- Peptide Nucleic Acid 292
- DNA with Extended Backbones: The Five-Atom Amide Linker 293
- Tetrose Nucleic Acid 293
- Homo-DNA 294
- Hexitol Nucleic Acid 296

TOOLS 296
- Seleno Nucleic Acids for Crystallographic Phase Determination 296
- Mirror Image DNA and RNA 297
- Neutron Macromolecular Crystallography 298

CONCLUDING REMARKS 298

INTRODUCTION

X-ray crystallography continues to be an important tool for investigating the structure and function of the nucleic acids. The ever-increasing number of structures deposited in databases bears witness to the central role that three-dimensional structural information plays in many areas of research, including chemistry, biology, medicine, material sciences, and the interfaces between them. Given the large range of functional topics addressed by the emerging structures, it makes sense to limit a review of recent crystallographic studies of nucleic acids to a specific area. Thus, we have decided to cover only recent crystal structures of chemically modified oligonucleotides and nucleic acid analogs in this article. Moreover, recent advances in nucleic acid crystallography were reviewed elsewhere (25), and other subjects, such as DNA bending (87), DNA-cation interactions (24, 45), noncanonical DNA structures (88), DNA-drug interactions (6), RNA folding motifs (42), ribozymes (17), and progress in the characterization of the structure and function of the ribosome (67), were the focus of review articles or edited books.

Ribozyme: RNA molecule that catalyzes a chemical reaction

Since the appearance of the review on current progress in nucleic acid crystallography (25) many new and exciting structures have been published, and we wish to list only a small selection here. The crystal structure of a junction between B-form and Z-form DNA revealed that conversion of the right-handed to the left-handed duplex form simply requires the breaking of a base pair and extrusion of the bases on each side (89). Hays et al. (41) investigated how DNA sequence affects structure based on the determination of nearly all possible structures of an inverted repeat sequence d(CCnnn$N_6N_7N_8$GG), where N_6, N_7, and N_8 are any of the four naturally occurring nucleotides and nnn are nucleotides required for self-complementarity. The crystal structure of a cytotoxic platinum(II) complex (TriplatinNC) bound to a DNA dodecamer duplex showed recurring square-planar coordination units (termed phosphate clamps), which consist of bidentate $N\cdots(P)O^-\cdots N$ complexes with phosphate oxygens (47b). The crystal structure of an RNA containing six CUG repeats was determined in order to probe the structural basis of myotonic dystrophy (61). The structure of a Diels-Alder ribozyme-product complex provided further evidence for RNA's functional versatility and revealed structural parallels in the active-site architectures of a catalytic antibody and the RNA enzyme, both of which

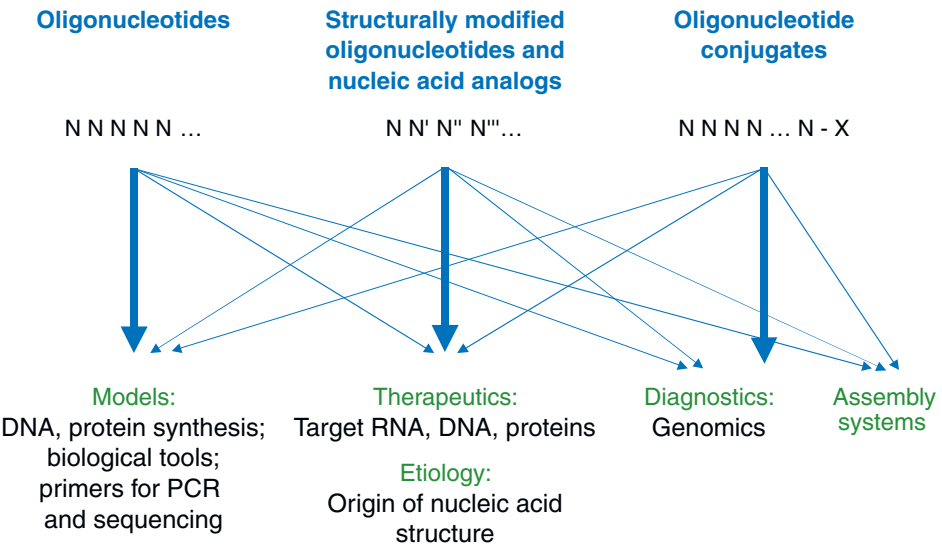

Figure 1

Diagram illustrating the versatile functions of synthetic oligonucleotides.

catalyze the carbon-carbon bond-forming reaction (86). Finally, the structure of the thiamine pyrophosphate (TPP) riboswitch from *Arabidopsis thaliana* with its regulatory ligand yielded insight into the reorganization of the riboswitch fold upon TPP binding and helped rationalize the mechanism of resistance to the antibiotic pyrithiamine (96).

One motivation to generate chemically modified oligonucleotides is their potential use as therapeutics. Thus, phosphorothioate DNAs (PS-DNAs) were evaluated as antisense agents against a wide range of targets (9, 10), and several of the so-called second-generation modifications have reached the clinical trial stage and are at various phases in the assessment of their therapeutic efficacy (7). However, the antisense community has witnessed many disappointments over the years regarding the performance of chemically modified oligonucleotides in the clinic. The advent of RNA interference (RNAi) has therefore energized the field, and the successful use of short interfering RNA molecules (siRNAs) to induce RNA degradation through a natural gene-silencing pathway has led to a revival of antisense technology (11). Although studies of RNAi therapeutic efficacy against a broad range of targets in rodents demonstrate the potential for RNAi for modulation of various diseases, in vivo delivery of siRNAs remains a significant obstacle.

An overview of potential applications of synthetic oligonucleotides is provided in **Figure 1**. From the diagram it is evident that drug discovery is just one of the motivations for chemical modification of nucleic acids. Chemically modified oligonucleotides have numerous other applications in chemistry, biochemistry, molecular biology, cell biology, diagnostics, nanotechnology and materials science, and are widely used as tools in genomics and target validation. Beyond serving more practical applications, modified nucleic acids play an important role as model systems to probe the structure and function of native DNA and RNA. Nucleic acid analogs that were generated for the purpose of a systematic investigation of an etiology of nucleic acid structure constitute examples in this regard (33). Our laboratory has a long-standing interest in the structural properties of chemically modified oligonucleotides (for an early review see Reference 21). Ongoing efforts have focused on conformational changes (22, 93, 101) as well as on secondary effects such as altered hydration (53, 90, 94) and metal ion binding (95) as a result of chemical

Phosphorothioate DNA (PS-DNA): DNA with one nonbridging phosphate oxygen replaced by a sulfur atom

Antisense: complementary to the sense (coding) strand; an approach whereby the sense strand is targeted with an artificial antisense oligonucleotide to downregulate protein synthesis

RNA interference (RNAi): a natural process leading to gene silencing via an RNA oligonucleotide duplex that triggers sequence-specific cleavage of a messenger RNA by the RNA-induced silencing complex

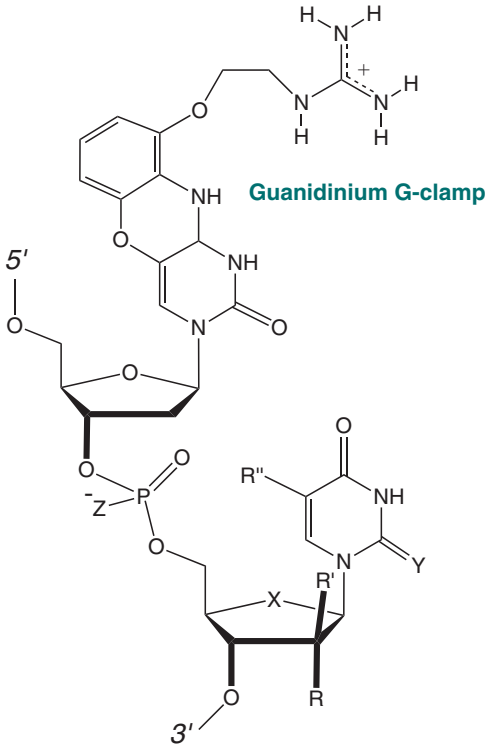

Figure 2

Chemical modifications of the nucleic acid sugar, base, and phosphate moieties. Sugar modifications: R = H, NH_2, OH, 2′-O substituents (see **Figure 3**), SeMe; R′ = OH (ANA), F (FANA); X = O, S. Base modifications: R″ = H, CH_3, various substituents at C5; Y = O, S. Phosphate modifications: Z = O (phosphate), S (phosphorothioate), Se (phosphoroselenoate).

modification. Detailed comparisons between a series of modifications concerning the same site (i.e., 2′-O-modified oligoribonucleotides) (27, 73, 79) and correlations between their three-dimensional structural properties and key features such as RNA affinity, nuclease resistance, and uptake were expected to yield guiding principles for the design of artificial nucleic acids with improved therapeutic efficacy compared with the first-generation PS-DNAs (23).

Here we review progress in the structural characterization of artificial oligonucleotide systems using X-ray crystallography in the past five years. In the section on the structural properties of nonnative oligonucleotide systems, we differentiate between chemically modified oligonucleotides and nucleic acid analogs. The first category includes, for example, oligonucleotides with 2′-carbohydrate modifications or conjugates with a stilbene moiety in place of a base pair. An overview of modification sites is given in **Figure 2**. Peptide nucleic acids and other systems such as homo-DNA, in which the pentose sugar is replaced by 2′,3′-β-D-dideoxyglucopyranose, i.e., pairing systems with more significant deviations from the familiar DNA and RNA frameworks, are classified as nucleic acid analogs.

siRNA: short interfering RNA

Nuclease: an enzyme that cleaves the sugar-phosphate backbone of a nucleic acid at internal (*endo*) or terminal (*exo*) sites

SUGAR MODIFICATIONS

Ribose 2′-O Modifications

The 2′ position of the DNA carbohydrate moiety is an attractive site for oligonucleotide modification for the purpose of antisense applications (56). The synthetic preparation of such analogs is relatively straightforward in many cases. Modification with an electronegative substituent locks the conformation of the sugar in the C3′-*endo* conformation and preorganizes the oligonucleotide for the RNA target strand (21, 22). The 2′ substituent can improve the chemical stability of the antisense oligonucleotide and protect it against attack by exo- and endonucleases. For example, the positively charged 2′-*O*-(3-aminopropyl) (2′-*O*-AP) modification confers excellent resistance against degradation by exonucleases (39) (**Figure 3** shows an overview of all 2′ modifications discussed in this section). In the crystal structure of the complex between the Klenow DNA polymerase I exonuclease and an oligonucleotide carrying 2′-*O*-AP-modified residues at its 3′ end, one of the metal cations required for catalysis was displaced from the active site by a salt bridge between the substituent's ammonium group and a carboxylate that is normally coordinated to the metal center (91). Further, 2′ modification can increase hydration of the minor groove and this results in higher affinity for RNA. The higher thermodynamic stability

of duplex RNA compared with DNA can be attributed in part to a stable minor groove water structure mediated by RNA 2′-hydroxyl groups (29). Another potential benefit of 2′ modification is the altered lipophilicity of an oligonucleotide that can affect uptake and lead to favorable pharmacokinetic properties.

Even a relatively simple modification such as 2′-*O*-methylation results in a significant increase in the melting temperature of the duplex compared to that of parent RNA (37). An initial crystal structure of a A-form DNA duplex with 2′-*O*-methylated adenosines had revealed water molecules bound to the 2′ oxygen and an antiperiplanar conformation of the C3′-C2′-O2′-CH_3 torsion angle (53) (see **Figure 3** for atom numbering). Therefore, it appeared that the higher stability brought about by 2′-*O*-methylation was not due to an entropically favorable release of water molecules from the minor groove. Indeed, subsequent molecular dynamics simulations of 2′-*O*-methylated RNA demonstrated stable hydration patterns around the hydrophobic moiety in the minor groove and residence times of water molecules that were extended compared with those bound to duplex RNA, consistent with a favorable enthalpic contribution to stability by 2′-*O*-methylation (3).

In the 2′-*O*-[2-(methoxy)ethyl] (2′-*O*-MOE) modification the conformational preorganization of the sugar extends into the substituent (90, 94). Most 2′-*O*-MOE substituents adopt a gauche conformation, and a water molecule trapped between O2′ and the methoxy oxygen is typically bridged to the adjacent phosphate group by either a single water molecule or a tandem of waters. It is reasonable to conclude that the increased hydration of the minor groove and the backbone in 2′-*O*-MOE RNA is at the origin of the favorable RNA affinity of this analog. Several 2′-*O*-MOE-modified oligoribonucleotides are now in clinical trials (7). The corresponding 2′-*O*-[2-(methylthio)ethyl] (2′-*O*-MTE) modification has enhanced binding to serum albumin, consistent with better uptake and biodistribution (77). Compared with 2′-*O*-MTE, the 2′-*O*-MOE modification exhibited poor binding to proteins but superior resistance to exonuclease degradation.

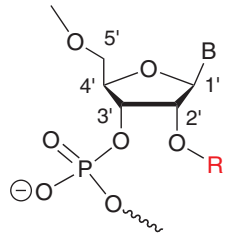

2′-*O*-Me:	R = CH_3
2′-*O*-AP:	R = CH_2-CH_2-CH_2-NH_3^+
2′-*O*-MOE:	R = CH_2-CH_2-O-CH_3
2′-*O*-MTE:	R = CH_2-CH_2-S-CH_3
2′-*O*-PRL:	R = CH_2-CH_2-CH_3
2′-*O*-BTL:	R = CH_2-$(CH_2)_2$-CH_3
2′-*O*-FET:	R = CH_2-CH_2F
2′-*O*-TFE:	R = CH_2-CF_3
2′-*O*-ALY:	R = CH_2-CH=CH_2
2′-*O*-PRG:	R = CH_2-C≡CH
2′-*O*-BOE:	R = CH_2-CH_2-O-CH_2-C_6H_5
2′-*O*-DMAOE:	R = CH_2-CH_2-O-$NH(CH_3)_2^+$
2′-*O*-DMAEOE:	R = CH_2-CH_2-O-CH_2-CH_2-$NH(CH_3)_2^+$
2′-*O*-MAOE:	R = CH_2-CH_2-O-N=CH_2
2′-*O*-IME:	R = CH_2-CH_2-Imidazole
2′-*O*-GE:	R = CH_2-CH_2-NH-C(NH_2)=NH_2^+
2′-*O*-NMC:	R = C(O)NH-CH_3
2′-*O*-NMA:	R= CH_2-C(O)NH-CH_3

Figure 3

Structures of 2′-*O*-sugar modifications that were studied in crystal structures of partially or fully modified oligonucleotides.

In order to try to combine the favorable RNA affinity of the 2′-*O*-MOE modification with the exceptional nuclease resistance of the 2′-*O*-AP modification, we designed the 2′-*O*-{2-[2-(*N*,*N*-dimethylamino)ethoxy]ethyl} (2′-*O*-DMAEOE) substituent (79) (**Figure 3**, **Figure 4*a***). Subsequent investigations showed that the optimal RNA affinity of MOE is preserved and that 2′-*O*-DMAEOE-modified oligonucleotides dodge degradation by exonucleases in a manner similar to those with 2′-*O*-AP modifications. The

Homo-DNA: synthetic, hexose-based nucleic acid in which the 2′-deoxyribose sugars of DNA are replaced by (4′→6′)-linked 2′,3′-dideoxy-β-D-glucopyranoses

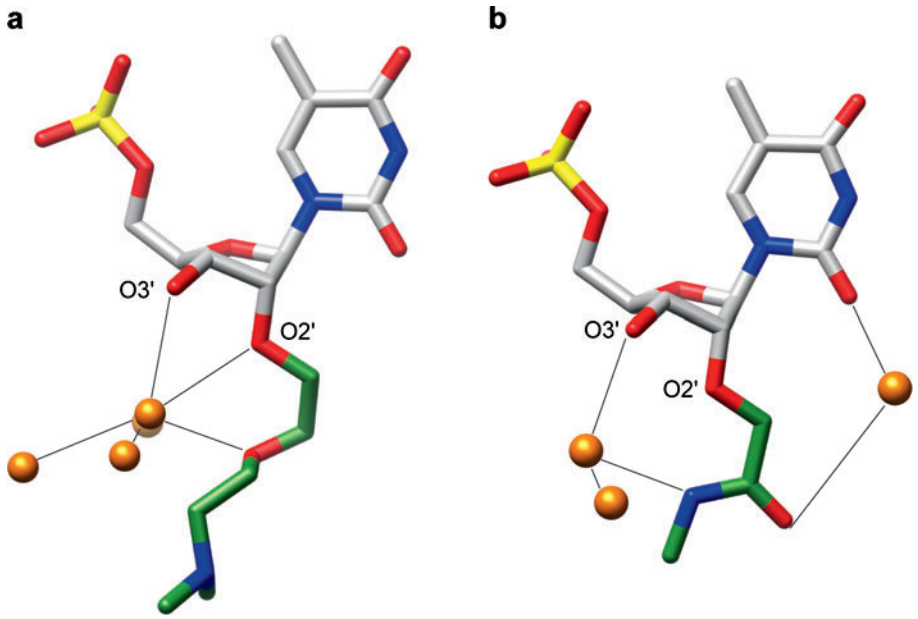

Figure 4

Conformation and hydration of (*a*) 2′-*O*-DMAEOE- and (*b*) 2′-*O*-NMA-modified nucleotides. Carbon atoms of 2′-*O* substituents are green and water molecules are orange spheres.

conformational preorganization of the DMAEOE substituent was confirmed by a crystallographic analysis of a modified duplex. Models of 2′-*O*-DMAEOE-RNA built on the basis of conformations of substituents in the crystal structure also helped rationalize an additional feature of this modification: Independent of whether substituents are consecutively placed or are dispersed throughout a strand, 2′-*O*-DMAEOE modification results in significantly increased RNA affinity. On the other hand, consecutive placement of zwitterionic substituents such as 2′-*O*-AP leads to diminished RNA affinity, potentially because of repulsion between substituents from adjacent residues. The above model confirmed that there are no steric clashes between adjacent 2′-*O*-DMAEOE substituents. Moreover, the conformational preferences of the DMAEOE substituent prevent close spacing of terminal *N*,*N*-dimethylamino moieties, which might result in electrostatically unfavorable interactions.

A further, zwitterionic modification, 2′-*O*-[2-(guanidiunim)ethyl] (2′-*O*-GE)-RNA, conferred excellent resistance against exonuclease degradation when placed at the 3′ end of antisense oligonucleotides (78). However, unlike the case of 2′-*O*-DMAEOE modification, consecutive placement of 2′-*O*-GE-modified residues led to a reduced increase in the RNA affinity per modification compared with oligonucleotides in which the modifications were dispersed. The crystal structure of a 2′-*O*-GE-modified A-form DNA duplex revealed that the guanidinium moieties were located near the phosphate group of the 3′-adjacent nucleotide (78). The resulting partial neutralization of the positive charge appears to be insufficient to prevent repulsive interactions between 2′-*O*-GE substituents in fully modified regions. By comparison, fully 2′-*O*-GE-modified strands exhibit high affinity for DNA duplexes, thereby providing an indication for effective interactions between positively charged substituents and negatively charged phosphate backbone.

We also conducted a comprehensive analysis of the RNA affinities, nuclease resistances, and structural properties of 10 additional 2′-*O* modifications: 2′-*O*-propyl (2′-*O*-PRL), 2′-*O*-butyl (2′-*O*-BTL), 2′-*O*-[2-(fluoro)ethyl] (2′-*O*-FET), 2′-*O*-[2-(trifluoro)ethyl] (2′-*O*-TFE), 2′-*O*-allyl

(2′-*O*-ALY), 2′-*O*-propargyl (2′-*O*-PRG), 2′-*O*-[2-(benzyloxy)ethyl] (2′-*O*-BOE), 2′-*O*-[2-(*N*,*N*-dimethylaminooxy)ethyl] (2′-*O*-DMAOE), 2′-*O*-[2-[(methyleneamino)oxy]-ethyl] (2′-*O*-MAOE), and 2′-*O*-[2-(imidazolyl)ethyl] (2′-*O*-IME) (27) (**Figure 3**). This work confirmed the importance of the electronegativity of the substituent and its conformational preorganization (i.e., via gauche effects between oxygen atoms as in the case of 2′-*O*-MOE) and hydration as factors for optimal RNA affinity. Positively charged substituents (i.e., 2′-*O*-DMAOE and 2′-*O*-IME) afforded better protection against nucleases than did smaller aliphatic or relatively short substituents with electron-withdrawing atoms. The better protection against nuclease attack conferred by some of the modifications appears to go along with close association of substituent and phosphate groups in the crystal structure. The 2′-*O*-BOE substituent led to better than expected RNA affinity, but oligonucleotides carrying this modification did not exhibit the resistance against nuclease degradation predicted for a relatively bulky modification. In the crystal structure, 2′ substituents are well ordered and conformational preorganization may account for the unexpected RNA affinity. On the other hand, the benzyl moieties are not in the vicinity of the phosphate groups and therefore may not sterically or electronically shield the backbone against a nuclease.

X-ray crystal structures also provided a rationalization of the significantly different RNA affinities observed for oligonucleotides bearing either 2′-*O*-[2-(methylamino)-2-oxoethyl] (2′-*O*-NMA)- or 2′-*O*-(*N*-methylcarbamate) (2′-*O*-NMC)-modified thymidines (73) (**Figure 3** and **Figure 4*b***). In the structure of the oligonucleotide with the destabilizing 2′-*O*-NMC modification, the NMC substituent forms a short contact with the sugar moiety (C1′) and an electrostatically unfavorable interaction with the exocyclic keto oxygen of the base. By comparison, in the structure of the oligonucleotide containing 2′-*O*-NMA-modified thymidines, the substituent's carbonyl oxygen engages in a water-mediated hydrogen bond to the base, and the nitrogen atom together with backbone O3′ stabilizes a water structure between the substituent and phosphate, reminiscent of that seen with the 2′-*O*-MOE modification (**Figure 4*b***).

2′-Amine-Substituted RNA

Substitution of the RNA 2′-hydroxyl group by an amine lowers the stability of duplex RNA but is beneficial in terms of nuclease resistance. This modification is more useful for analyzing RNA structure and RNA-ligand interactions than for antisense applications (19, 98). Crystal structures of RNA 16mer duplexes with 2′-amino-C paired with either G or A demonstrated that the substitution is well tolerated in the A-form duplex (38). Similarly, a 2′-amide product generated by acylation of the amine is compatible with a standard duplex geometry. The amine acylation transition state was simulated by the structure of a 2′-amino-C-containing RNA at pH 5. Under these conditions the 2′-amine group is protonated, and in the crystal structure the 3′-phosphodiester moiety moved toward the amine and the modified nucleotide was rotated into the minor groove. These conformational adjustments bring the 2′-amino group within hydrogen bonding distance of the bridging 5′-phosphodiester oxygen, supporting the conclusion that 2′-amine acylation proceeds most efficiently when the base is flipped out of the helix or when it forms a mismatch pair.

Arabinonucleic Acid and 2′-Deoxy-2′-Fluoroarabinonucleic Acid

Recognition by RNase H of the hybrid duplex formed between an antisense oligonucleotide and its target RNA is considered of crucial importance for the efficacy of a particular nucleic acid modification (52, 99). Unfortunately,

ANA: arabinonucleic acid

FANA: 2′-deoxy-2′-fluoroarabinonucleic acid

only a handful of modifications, including PS-DNA, arabinonucleic acid (ANA) (**Figure 2**), and 2′-deoxy-2′-fluoroarabinonucleic acid (FANA), elicit RNase H action (12). However, none of the above 2′-carbohydrate modifications are tolerated by the enzyme unless they are applied as mixed oligomers with central PS-DNA windows. The enzyme binds to double-stranded RNA and RNA:DNA hybrids from the minor groove side, and the intolerance toward many modifications is due likely to steric conflicts in the minor groove. In addition, it was long suspected that the width of the minor groove of the hybrid duplex would play a key role in substrate recognition (36, 65). The minor groove of a hybrid duplex, in which the riboses adopt a C3′-*endo* (North) pucker and the 2′ deoxyriboses adopt either a C2′-*endo* (South) (36) or an O4′-*endo* (East) (60) pucker, is contracted relative to a canonical A-form. Double-stranded RNAs are not cleaved by RNase H. In the recently determined crystal structure of a bacterial RNase H bound to an RNA:DNA hybrid, sugars in the RNA strand exhibited the expected C3′-*endo* conformation and sugars in the DNA strand at the enzyme active site adopt a C2′-*endo* pucker (68). The minor groove of the duplex was indeed narrower than a standard A-form double helix.

In a B-form duplex environment, FANA-T adopted an O4′-*endo* sugar conformation (4), and subsequent crystal structures of A-form DNA duplexes containing single ANA or FANA residues and of B-form DNA duplexes with incorporated ANA residues provided good evidence for different conformational preferences by ANA and FANA (51). Thus, sugar puckers of FANA residues are restricted to the North-East quadrant of the pseudorotation phase cycle (C3′-*endo* and C4′-*exo* in the A-form and O4′-*endo* in the B-form duplex environments). Sugar puckers of ANA residues are restricted to the South-East quadrant (O4′-*endo* and C1′-*exo* in the B-form and C1′-*exo* in the A-form duplex environments). The latter observation is unexpected, as the C1′-*exo* pucker of ANA residues in the A-form duplex distorts the geometry locally, unlike an O4′-*endo* conformation of a sugar in a B-form DNA duplex. The observed conformations of ANA and FANA residues are unlikely to be induced by the particular geometry of the DNA duplex in which they were studied.

Another difference between ANA and FANA is the absence of water molecules around the fluorine atom in FANA, whereas the hydroxyl group of ANA is well hydrated in the crystal structures. In both cases the 2′ substituents are located in the major groove, thus precluding any steric conflicts with residues from the enzyme active site. FANA's affinity for RNA significantly exceeds that of ANA (100), indicating that the conformational preorganization afforded by the 2′-fluorine substituent is stronger than the combined effects of preorganization by the 2′-OH and favorable contributions to the stability of ANA:RNA duplexes by the 2′-OH-mediated water structure.

The finding that FANA's conformational preferences are not compatible with a South-type sugar pucker begs the question of the particular geometry of the FANA:RNA duplex at the active site of RNase H. Because it is unlikely that the FANA strand will be forced into a C2′-*endo* conformation, it is possible that the enzyme tolerates a limited range of conformations in the strand paired to RNA (i.e., O4′-*endo*). A crystal structure of the enzyme in complex with a FANA:RNA substrate duplex may help answer this question in the future.

4′-Thio-RNA

Substitution of nucleic acid oxygen atoms by sulfur is conducive to the generation of antisense modifications. In addition to the well-known first-generation PS-DNA, 4′-thio-RNA (**Figure 2**) has recently been investigated in terms of its RNA affinity and nuclease resistance and suitability for siRNA and aptamer applications (57). Several approaches for the synthesis of fully modified 4′-thio-RNAs have been presented (40, 44).

The modification increases resistance against exo- and endonuclease attack, and duplexes between 4′-thio-RNA strands are significantly more stable thermodynamically than RNA duplexes. Compared with the crystal structure of the native duplex, the crystal structure of an RNA duplex with an isolated 4′ thiocytosine per strand showed only minor geometrical deviations (40). The 4′ thioribose adopts a standard C3′-*endo* pucker, although the sugar is more bulky owing to extended C1′-S and S-C4′ bond lengths compared with the natural ribose. The structure allowed only limited conclusions with regard to the consequences of the 4′-thio substitution for backbone and groove hydration. Crystals of a fully 4′-thio-modified RNA duplex that diffract X-rays to medium resolution are available in our lab but have resisted structure determination efforts thus far (M. Egli & P.S. Pallan, unpublished data). Recently, the synthesis and pairing properties of all 4′-thio-DNAs have been published (47). Accordingly, 4′-thio-DNA exhibits excellent resistance to degradation by exo- and endonucleases, and its hybridization and structural properties resemble those of RNA.

BASE MODIFICATIONS

Compared with studies of modifications of the sugar moiety, there are only very few studies of crystal structures of oligonucleotides containing base analogs. Many investigations concerning artificial bases or base pairs have focused on DNA's four-letter alphabet for biological information storage (62, 69, 76). Could this alphabet be extended, or is it possible to create alternative coding systems using either altered hydrogen bonding patterns or hydrophobic interactions in place of the well-known Watson-Crick hydrogen bonding? For example, nucleotides containing complementary pyridine-2,6-dicarboxylate (Dipic) and pyridine (Py) bases formed stable and selective Cu^{2+}-mediated pairs, and the crystal structure of a decamer DNA duplex with a single Dipic-Py pair confirmed the square-planar coordination mode of Cu^{2+} in the plane of the Dipic base (2). Base analogs were also used to probe the role of individual bases or functional groups in the core region of the hammerhead ribozyme, and the crystal structure of a hydrophobic analog, a ribonucleoside with a phenyl in place of the base moiety, was analyzed in the context of an RNA duplex (59). Two phenylribonucleosides formed a pseudopair in the center of the duplex, apparently preferring this arrangement to the expected pairing with G.

The natural nucleobases were also modified in order to enhance stacking or to increase hydrogen bonding strength, for example, through the introduction of cationic tethers in the cytosine analog guanidinium G-clamp (101) (**Figure 2**). Simple replacement of the O2 oxygen by sulfur in the 2-thiothymine (m^5s^2U) analog was observed to stabilize a C3′-*endo* conformation of the sugar and, when combined with the 2′-*O*-MOE modification, to furnish high affinity for RNA and nuclease resistance (15). Therefore, substitution of oxygen by sulfur in the phosphate (PS-DNA), sugar (4′-thio-RNA), or base moieties (m^5s^2U) has led to analogs with attractive properties for antisense and siRNA applications. The following paragraphs provide brief summaries of other crystallographic studies involving oligonucleotides with incorporated base analogs.

Base Analogs with Cationic Tethers

Introduction of a single tricyclic cytosine analog 9-(2-guanidinoethoxy)-phenoxazine (guanidinium G-clamp) (**Figure 2**) into DNA strands leads to a dramatic increase of ∼16°C in the melting temperature of the duplex with an RNA strand (101). The analog was designed to allow for the formation of Hoogsteen-type hydrogen bonds by amino and imino nitrogens of the positively charged guanidinium moiety to the O6 and N7 atoms of G in the major groove. This binding mode was inspired by the major groove Arg···G interaction present in virtually all

CPD: cyclobutane-type pyrimidine photodimer

structures of protein complexes (e.g., 74). The crystal structure of an A-form DNA decamer fragment with two guanidinium G-clamp:G base pairs at high resolution confirmed the formation of five hydrogen bonds between the analog and G (101). The impressive stability gains afforded by the G-clamp are not simply a result of the two additional Hoogsteen hydrogen bonds and favorable electrostatics, owing to the placement of a positive charge into a region of strong electronegative potential. They are also due to better stacking and a stable water structure that links the guanidinium moiety to the 5′- and 3′-phosphate groups of G on the opposite strand. In addition, the guanidinium G-clamp fits almost seamlessly into the duplex, and apart from minor local changes in the base parameter buckle, propeller twist, and opening angle, there were no notable deviations compared with a reference structure without the C analog that was determined to a similar resolution (101).

Potential roles of cations in the modulation of DNA duplex conformation were probed by inserting thymidines carrying an *N*-propylamine at the 5′ position (64). The crystal structure of $[d(CGCGAAXXCGCG)]_2$, where X is the T analog with the tethered amine, revealed that three of the cationic linkers were pointing away from the DNA duplex. The fourth linker assumes an orientation that brings it in relatively close association with the backbone, and the tethered ammonium ion interacts with a phosphate group on the 3′ side of the modified T. This electrostatically favorable interaction is accompanied by alterations in rise, roll, and twist angles and a shift of the backbone relative to the unmodified oligonucleotide duplex. In addition, the presence of the tethered ammonium ion at that location is associated with displacement of counterions (Mg^{2+}, Tl^{+}) from the major groove.

Oligonucleotides containing 5-(*N*-aminohexyl)carbamoyl-modified uracils (^{N}U) and the 2′-*O*-methylated ^{N}U analog were tested for their affinities for DNA and RNA, respectively (47a) (**Figure 2**). Both modifications bring about substantial gains in affinity for their respective targets and enhance resistance to nucleases. Crystal structures of DNA:DNA and DNA:RNA duplexes containing ^{N}U analogs in the DNA strand demonstrate that a hydrogen bond between the carbamoyl amino group and O4 of uracil fixes the aminohexyl chains in the major groove. The terminal ammonium groups of the substituents can form salt bridges to phosphate groups of the target strand, consistent with the increased RNA affinities of DNA strands with incorporated 2′-*O*-methylated ^{N}U residues.

Cis-syn Thymine Dimer

Given that the cyclobutane-type pyrimidine photodimer (CPD) is the most abundant lesion as a result of UV-induced DNA damage and constitutes a major cause of skin cancer, it is perhaps surprising that only in 2002 the first and only crystal structure of an unbound oligodeoxynucleotide (in the absence of protein) containing a CPD was determined (72). The 3′ thymine of the CPD maintains Watson-Crick hydrogen bonds with the complementary A. However, only one hydrogen bond is observed between the 5′-T(CPD) and A (the O4 · · · N6 hydrogen bond is about 0.6 Å longer than expected). The presence of the CPD leads to roll-bend of about 30° into the major groove near the center of the decamer DNA duplex. In addition, the duplex is unwound by about 9° in the region of the lesion and the major and minor grooves on both the 3′ and 5′ sides of the CPD are enlarged. The structure provides an indication of some of the topological changes that the repair machinery may use for damage sensing and processing.

DNA Conjugates with Stilbene-Diether Linkers

Synthetic DNA conjugates with bis(2-hydroxyethyl)stilbene-4,4′-diether (Sd2) linkers can fold into stable hairpins that are capped

by the stilbene moiety. In fact they constitute the thermodynamically most stable DNA hairpins characterized to date: Even a simple stem of two C:G base pairs with an Sd2 cap melts at >80°C in a buffered solution containing 0.1 M NaCl (49). A related linker, stilbenedicarboxamide (Sa) in the excited singlet state, acts as a selective electron acceptor that oxidizes G but none of the other DNA bases. This property permitted an investigation of hole injection and migration processes in DNA hairpins (50). On the other hand, in DNA hairpins containing Sd2 caps the singlet state of the stilbene linker is an electron donor that reduces T or C but not A or G. In the low-resolution crystal structure of the hairpin d(GT_4G)-Sd2-d(CA_4C), the stilbene moiety stacked on the adjacent C:G base pair (49). Packing interactions included a pinwheel-like arrangement involving four neighboring hairpin molecules with edge-to-face interactions between adjacent stilbene moieties.

A subsequent structure at 1.5 Å resolution of the same Sd2-conjugated DNA revealed two independent molecules per asymmetric unit with altered interactions in the crystal lattice (30). In one of the hairpins the stilbene moiety was stacked on the C:G base pair below (**Figure 5**). In the other hairpin the stilbene adopted a twisted conformation, whereby one phenyl ring of Sd2 was unstacked from the G and the other assumed an edge-to-face orientation with C. Thus, the structural data indicate conformational flexibility of the stilbene cap in DNA hairpins, consistent with facile transition between face-to-face and edge-to-face π-π interactions and *cis-trans* conversion of the stilbene. These structures also provide a nice demonstration for altered packing interactions (i.e., absence of end-to-end stacking between adjacent duplexes) in DNA crystals as a result of chemical modification. An additional interesting feature of the structure of the Sd2-conjugated DNA was the observation of Mg^{2+} hexahydrate coordination in the minor groove of the A-tract. Sequences with runs of A:T pairs that are uninterrupted by a TpA step exhibit particularly narrow minor grooves (24, 45). Remarkably, Mg^{2+} coordination led to further contraction of the minor groove in the A-tract of the Sd2-capped DNA hexamer duplex (30).

DFT: 2,4-difluorotoluene (apolar thymine analog)

Difluorotoluene Analog of T

In addition to serving as a probe for the relative importance of hydrogen bonding and shape of nucleobases in DNA replication (62), the difluorotoluene analog of T (DFT) has also been incorporated into siRNAs in its ribonucleoside form (rDFT). Incorporation of rDFT at the 5′ end of the guide strand did not affect gene silencing compared with unmodified RNA (104). Similarly, internal substitutions of U by rDFT were well tolerated. The melting temperatures of RNA duplexes bearing A:DFT pairs were reduced compared with native RNA duplexes, but the former duplexes

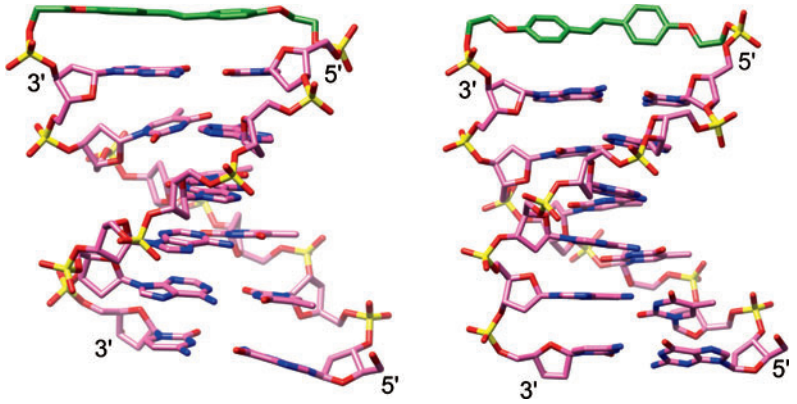

Figure 5
Comparison of DNA hexamer duplexes capped by stilbenediether linkers (Sd2, *green*) with face-to-face (*left*) and edge-to-face (*right*) orientations relative to the adjacent G:C base pair.

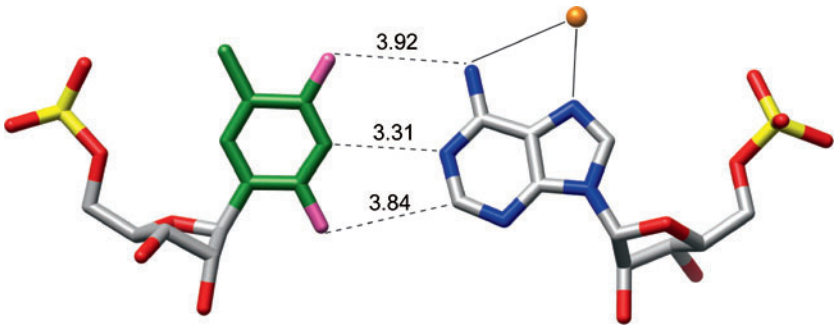

Figure 6

Structure of an RNA difluorotoluene (rDFT):A base pair with distances shown in Ångstroms.

were more stable than corresponding RNAs with base mismatches. The crystal structure of an RNA dodecamer duplex with two rDFT:A pairs at high resolution revealed that DFT and A were more loosely associated than a standard U:A pair (104). The (DFT)F · · · N6(A) distances were 3.78 and 3.92 Å in the two pairs and thus about 1 Å longer than Watson-Crick O4(U) · · · N6(A) hydrogen bonds (**Figure 6**). Moreover, DFT:A pairs exhibited opening, strong rolling, and shearing, consistent with the larger distance between DFT and A and the absence of hydrogen bonds between them [except for a relatively weak (DFT)C-H · · · N1(A) interaction]. Remarkably, DFT:G pairs in the crystal structure of another RNA duplex showed much shorter distances between F and the N1-H function of G (M. Egli & L. Feng, unpublished data). This structure demonstrates that organic fluorine can engage in short contacts with hydrogen bond donors. However, replacement of C by rDFT (leading to DFT:G wobble pairs) was not tolerated in siRNAs and abolished gene silencing by the RNA-induced silencing complex (104).

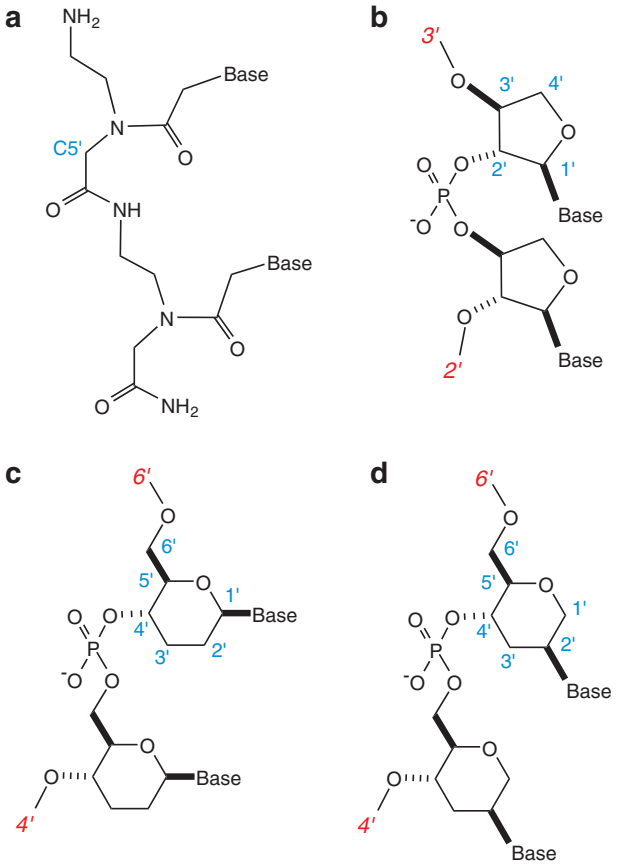

Figure 7

Structures of (*a*) PNA, (*b*) TNA, (*c*) homo-DNA, and (*d*) HNA.

NUCLEIC ACID ANALOGS

Peptide Nucleic Acid

Several new structures of peptide nucleic acid (PNA) molecules have recently been reported. Peptide nucleic acid is a synthetic DNA mimic in which the phosphodiester backbone is replaced by *N*-(2-aminoethyl) glycine units and with a methylene carbonyl moiety linking nucleobases and polyamide backbone (66) (**Figure 7*a***). PNA is achiral, shows stable self-pairing, and cross-pairs with DNA and RNA, and structures have shown the formation of

left-handed and right-handed, so-called P-form helices (20). The PNA duplex features a wide and deep major groove, a twist of ~20° (18 base pairs per turn), and a rise of ~3.4 Å, whereby the base pairs are perpendicular to the helix axis. Introduction of an L-lysine at the C terminus appears to lead to a preference for a left-handed helix by the PNA double strand in solution. However, in the structure of the PNA hexamer H-CGTACG-L-Lys-NH_2, both left- and right-handed duplexes were observed (81). The structure deviated only minimally from that of the unmodified strand (80), indicating that the addition of lysine did not affect the geometry of the P-form helix. Apparently, packing interactions in the crystal prevent induction of the left-handed duplex, which is thought to be preferred in solution because of a favorable free energy of hydration as a result of the cation-π interaction between lysine and the terminal guanine base (81).

Similarly, in the structure of the PNA decamer H-GTAGATCACT-L-Lys-NH_2 with the same C-terminal lysine modification, both left- and right-handed helices were observed (75). However, each PNA strand contains a left- and a right-handed section, and together with the overhangs this leads to the formation of a PNA triplex through Hoogsteen-type base pairs. PNA was also modified with lysine internally. For example, the structure of a decameric PNA with a segment of lysine-PNA (side chain in the D configuration attached to C5′) (**Figure 7*a***) paired to DNA was determined at high resolution (58). The PNA-DNA hybrid assumes a right-handed P-helix geometry with about 16 base pairs per turn. The similarities between the PNA:DNA and PNA:PNA duplexes demonstrate that PNA is conformationally rigid and has an intrinsic preference for the P-form helix.

DNA with Extended Backbones: The Five-Atom Amide Linker

DNAs with incorporated 2′-deoxyribonucleoside dimers that are connected by a five-atom linker O3′-CH*(CH_3)-CO-NH-CH_2 (*designates a chiral center) in place of the standard DNA and RNA four-atom linker O3′-P-O5′-C5′ were found to exhibit RNA affinities that were only slightly reduced compared with native oligodeoxynucleotides (13). This finding prompted us to synthesize DNA strands with incorporated dimers linked by five-atom amides of the type X3′-C*H(CH_3)-CO-NH-CH_2 (X = O, CH_2). Particularly in cases in which the extended backbone was combined with a 2′-methoxy modification of the 3′ sugar in the dimer, slight increases were seen in the RNA affinity of DNAs carrying single or multiple amide-linked dimers compared to native DNA or DNA strands with 2′-methoxy modifications (71). Judging from circular dichroism (CD) experiments in solution, no drastic deviations from the conformations of the native DNA:RNA hybrids result upon incorporation of amide-linked dimers. Moreover, a crystal structure of a hybrid duplex between an RNA nonamer and a DNA with a single amide-linked dimer did not reveal any significant deviations compared with the structure of the unmodified DNA:RNA hybrid, i.e., disruption of stacking at or near the site of the extended backbone. Thus, different types of nucleic acids undergo stable cross-pairing even though the numbers of backbone atoms linking their residues do not match.

Peptide nucleic acid (PNA): synthetic DNA mimic featuring a polyamide backbone that is linked to nucleobases via a methylene carbonyl moiety

TNA: (L)-α-threofuranosyl-(3′→2′) nucleic acid

Tetrose Nucleic Acid

The (L)-α-threofuranosyl-(3′→2′) nucleic acid (TNA) system (**Figure 7*b***) was investigated within the context of an etiology of nucleic acid structure (32, 33). TNA forms stable duplexes with itself and, despite having a shorter backbone than DNA and RNA, is able to cross-pair with both (84). The sugar puckers in RNA and B-form DNA duplexes differ (C3′-*endo* versus C2′-*endo*, respectively), and the distance between adjacent intrastrand phosphate groups in the former is about 1 Å shorter (6 versus 7 Å, respectively) (82). TNA

possesses a higher affinity to RNA than to DNA. Crystal structures of A-form (70) and B-form DNA duplexes (103) containing TNA residues revealed that the α-threofuranose sugar uniformly adopts a C4′-*exo* pucker with a quasi-diaxial orientation of the 2′ and 3′ substituents. The diameter of the B-form duplex was slightly contracted at the site of the TNA modifications to accommodate the shorter backbone of the TNA thymidines. However, helical rise and twist were virtually unchanged at the site of the TNA residues compared with a native DNA reference duplex and hence stacking was unaffected by the presence of a single TNA nucleotide per strand (103). However, a comparison with the conformation of the TNA nucleoside in the A-form duplex showed that, independent of the environment, the P···P distance is nearly the same (5.79 Å in B-form duplex versus 5.70 Å in A-form duplex). This indicates that the shorter backbone of TNA is unable to expand to a distance of ∼7 Å between the 3′- and 2′-phosphate groups, typically encountered in B-form DNA (between the 5′ and 3′phosphates). Therefore it is likely that DNA adapts to the conformational constraints of TNA and not vice versa.

Overall, the structural data support the conclusion that TNA's higher affinity for RNA than for DNA is due to the closer conformational correspondence of TNA and RNA (70). DNA is unique in its ability to switch between duplex states with either C2′- or C3′-*endo* sugar puckers, and it is more likely that DNA adapts conformationally to TNA than the other way around. Pairing between nucleic acid species with different geometries of the backbone is certainly possible (as demonstrated by PNA as well as the above DNAs with extended amide-linked backbones). However, duplexes between nucleic acids of different constitution but with similar spatial and conformational properties can be expected to be of higher stability than duplexes formed by pairing partners that don't exhibit a close geometric match. DNA and RNA constitute an obvious example in this regard because of the generally lower thermodynamic stability of DNA:RNA hybrids relative to that of RNA:RNA duplexes.

Homo-DNA

(4′→6′)-Linked oligo(2′,3′-dideoxy-β-D-glucopyranosyl)nucleotides (homo-DNA) (**Figure 7*c***) represent the earliest model system investigated in studies by Eschenmoser and colleagues directed at an etiology of nucleic acid structure. Its synthesis and an assessment of the pairing properties were motivated by the question, "Why pentose and not hexose nucleic acids?" (34, 35). Unlike TNA, homo-DNA constitutes an autonomous pairing system; therefore homo-DNA strands do not pair with any of the known nucleic acid systems (i.e., DNA, RNA, or PNA). However, homo-DNA duplexes are thermodynamically more stable than DNA duplexes of the same sequence, and the pairing priorities are altered in homo-DNA as a result of the hexose-phosphate backbone: G:C > A:A ≈ G:G > A:T (DNA: G:C > A:T) (46). The higher stability is entropy based and consistent with the reduced flexibility of the hexopyranose sugar than with the pentofuranoses in DNA and RNA. Homo-DNA pairing is strictly antiparallel and purine-purine pairing is of the reverse-Hoogsteen type. (4′→6′)-Linked nucleic acid systems based on fully hydroxylated hexopyranoses, such as oligo-β-D-glucopyranosylnucleotides, oligo-β-D-allopyranosylnucleotides, and oligo-β-D-altropyranosylnucleotides, are unable to pair (32). Neither a qualitative conformational analysis of homo-DNA (34) nor any of the subsequently proposed three-dimensional models of homo-DNA duplexes allowed definitive conclusions regarding its geometry (i.e., duplex helical rise and twist and repeats per turn; reviewed in Reference 26). The recently determined crystal structure of the homo-DNA octamer dd(CGAATTCG) (dd = 2′,3′-*did*eoxygluopyranose) at 1.75 Å resolution has finally provided a detailed

picture of the geometry of the homo-DNA duplex and an improved answer to the question, "Why pentose and not hexose nucleic acids?" (28).

Unlike the tightly wound double helix known from B-form DNA, the octamer duplex $[dd(CGAATTCG)]_2$ resembles a slowly writhing, right-handed ribbon (**Figure 8**). Hallmarks of the duplex are (*a*) the steep angle between the hexose-phosphate backbones and base axes, (*b*) the virtual absence of intrastrand stacking and the presence of extensive overlaps between bases from opposite strands, (*c*) a chair conformation of the hexose, (*d*) an average helical rise of 3.8 Å (high 5.1 Å, low 2.9 Å), (*e*) highly irregular twist angles (average 14°, high 92°, low 0°), and (*f*) relatively closely spaced phosphate groups in each strand (average P···P distance 5.8 Å). The range of helical rise and twist values provides an indication of the irregular geometry of the duplex. Unlike the two DNA strands that wind around each other gracefully and in a highly repetitive fashion, the homo-DNA duplex has a more haphazard appearance. Remarkable in this context are the absence of twisting at the outer CpG and the central ApT base-pair steps and the overlap of cross-strand cytosines and adenines in the former and the latter, respectively (**Figure 8**). The first of the two adenines in both strands is pulled out from the stack and inserted into an adjacent duplex, whereby pairs of duplexes cross each other at an angle of ~60° (**Figure 8**). Looped-out adenines form reverse-Hoogsteen base pairs with thymidines from the crossing duplex, consistent with the earlier observation of facile purine:purine pairing between strands that assume an antiparallel orientation (46).

The strong positive slant (average 44°) (28) between backbone direction and base planes in homo-DNA is readily apparent because the duplex is unwound, giving it the appearance of an inclined ladder with uneven spacing of rungs. The strong twist of DNA and RNA duplexes obscures the fact that the two duplexes feature different inclinations between backbones and base planes. In DNA, the backbone

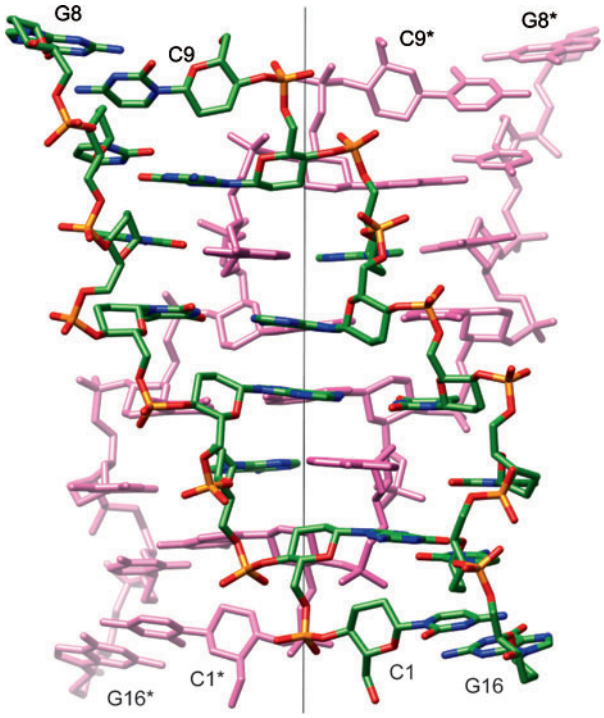

Figure 8

Dimerization of homo-DNA duplexes around a crystallographic dyad (*thin gray line*). The duplex in the foreground is viewed across the minor groove and the symmetry mate is pink.

is virtually normal to the base axes (inclination angle 0°), but in RNA the backbone has an inclination of ~–30° (26, 28). Each nucleic acid system exhibits a unique base-backbone inclination angle, and the fact that bases and backbones in DNA assume a roughly perpendicular relative orientation provides the basis for its ability to form parallel-stranded duplexes. On the other hand, RNA and homo-DNA that have significant inclination angles can pair only in an antiparallel fashion. Apart from restraining the relative polarity of strands, the difference between the inclination angles of two nucleic acid systems can also serve as an indicator of the potential for pairing between the two. Thus, DNA can adapt to the inclination of RNA (B-form to A-form DNA transition), forming the basis for DNA:RNA hybridization. Conversely, the strongly different inclinations between DNA and homo-DNA and between RNA and homo-DNA prevent

HNA: 2′,3′-dideoxy-1′,5′-anhydro-D-arabino-hexitol nucleic acid

pairing between homo-DNA and either of the natural nucleic acids.

In addition to providing insights into fundamental issues of nucleic acid chemistry and biology, such as relative strand polarity and base-pairing priorities, the structure of homo-DNA also shed light on the absence of pairing with fully hydroxylated hexopyranosyl nucleic acids (i.e., glucose, allose, and altrose nucleic acids). Thus, the addition of hydroxyl groups in the various configurations to the C2′ and C3′ positions of the 2′,3′-dideoxyglucopyranose in the homo-DNA structure produces various short contacts between adjacent sugars as well as between sugar and base and sugar and phosphate oxygens. Therefore, the homo-DNA structure helps rationalize nature's preference for pentose to hexose in the genetic system.

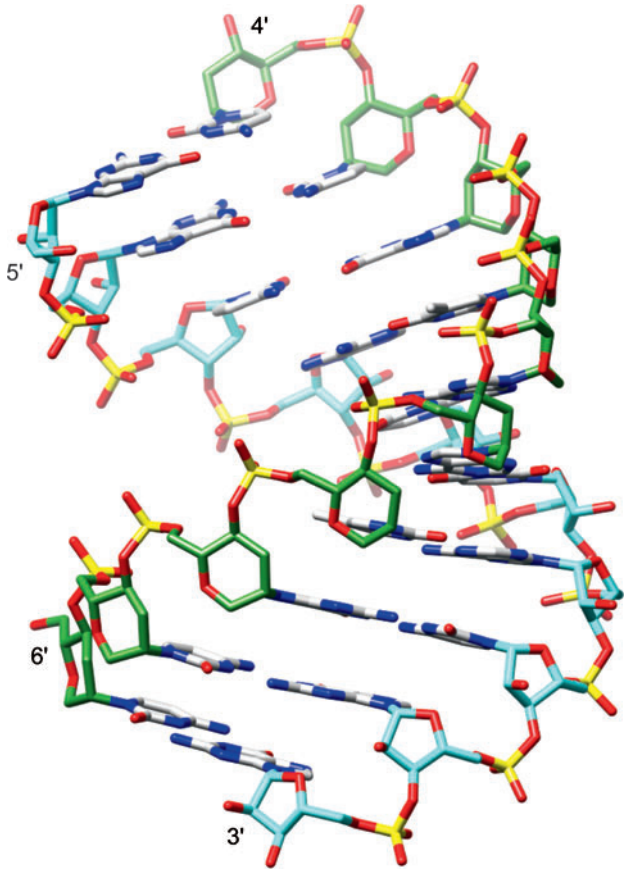

Figure 9

Crystal structure of an A-form-like HNA:RNA hybrid duplex viewed across the major (*left*) and minor (*right*) grooves. Carbon atoms of hexitol and ribose sugars are green and cyan, respectively.

Hexitol Nucleic Acid

The 2′,3′-dideoxy-1′,5′-anhydro-D-arabino-hexitol nucleic acid (HNA) system (**Figure 7*d***) represents another analog in which the five-membered sugar ring of DNA is replaced by a hexose (14). HNA is being studied as a promising antisense modification, and unlike homo-DNA, with which it shares the 4′→6′-phosphodiester internucleotide linkages, it forms stable duplexes with RNA and DNA. Based on melting temperature measurements, the order of duplex stability is as follows: HNA:HNA > HNA:RNA > HNA:DNA. The preference for DNA to RNA is consistent with an A-form-like conformation of the HNA double helix, as established by X-ray crystallography (14). As expected, all hexoses show a chair conformation, in line with the higher conformational preorganization of HNA than with DNA. However, a recent crystal structure of an HNA:RNA duplex (**Figure 9**) at 2.6 Å resolution revealed four independent molecules per asymmetric unit that exhibit some conformational variations in their HNA strands (55). These structures also disclosed a reinforced hydration of HNA phosphate groups that might contribute to the high stability of HNA duplexes and hybrids between HNA and DNA or HNA and RNA. This observation once again confirms hydration as an important player in nucleic acid stability and function.

TOOLS

Seleno Nucleic Acids for Crystallographic Phase Determination

Molecular replacement is typically the method of choice for structure determination

of double-helical nucleic acid fragments. However, many structures do not yield to this approach; chemical modification often results in conformational changes that render futile the use of models with canonical geometry. Normally, one then resorts to brominated fragments (Br^5U or Br^5C) in combination with the multiwavelength anomalous dispersion technique to generate phases. Although often successful, bromo derivatives have a number of disadvantages. For example, nucleotides brominated at the 5′ position of pyrimidines are photolabile, and exposure of derivative crystals to medium- and high-intensity X-rays can result in the loss of bromine (31). Moreover, crystals from brominated oligonucleotides often diffract X-rays to lower resolution than do crystals from native molecules; in some instances brominated strands do not yield crystals. For example, none of the homo-DNA octamers dd(CGAATTCG) modified with either a single Br^5U or a single Br^5C provided crystals, thus precluding application of multiwavelength anomalous dispersion phasing (26, 28). To determine the structure of homo-DNA, we used a single phosphoroselenoate derivative (26, 28) (**Figure 2**), an approach that was first tested with crystals of a left-handed Z-form DNA hexamer fragment (102). Selenium can also be incorporated at the 2′ position of the ribose moiety in the form of 2′-methylselenonucleosides (18) (**Figure 2**). A proof of principle study using this phasing approach was initially carried out for an A-form DNA fragment (92). However, this method is particularly suited for RNA crystallography (63, 86) and has been extended to long RNAs (43).

Mirror Image DNA and RNA

There are more possibilities for favorable packing arrangements in racemic space groups than in the 65 chiral space groups (from a total of 230). According to a survey carried out approximately 15 years ago (5), about 90% of the small-molecule compounds that can crystallize in either racemic or chiral space groups prefer the former. This preference need not be a result of particular interactions between the enantiomers in the crystal but may simply be related to the greater variety of packing molecules in racemic space groups. However, there remains the possibility that racemic crystals also exhibit greater density and thermodynamic stability than their chiral counterparts (5 and references within).

Crystallization and structure determination of racemic mixtures of D- and L-oligonucleotides have been reported in only two cases. A 1:1 mixture of D- and L-d(CGCGCG) crystallized in space group *P*-1, and the structure was determined to 2.2 Å resolution (16). However, crystals of D-d(CGCGCG) Z-form DNA with space group $P2_12_12_1$ diffract X-rays to exceptionally high resolution (>0.6 Å) (95). The structure of the racemic crystal of the RNA octamer duplex r(CUGGGCGG):r(CCGCCUGG) was determined to 1.4 Å resolution (83). But chiral crystals based on the RNA L-isomers alone were also obtained and reported to diffract to a resolution of 1.9 Å (97). On the basis of these two cases it is impossible to judge whether the use of racemic mixtures may significantly increase the chances for growing crystals of nucleic acid fragments. All four of the above structures feature end-to-end stacking between neighboring helices and the formation of infinite columns. Thus, there are no fundamental differences between chiral and racemic crystals in terms of packing motifs. Our own experience regarding the use of racemic mixtures of oligonucleotides to facilitate crystallization was rather disappointing. In the mid-1990s we conducted crystallization trials with chiral and racemic mixtures of DNA and RNA dodecamers. Whereas chiral crystals of D-d(CGCGAATTCGCG) diffract to atomic resolution, no crystals were obtained for the racemic mixture. Neither the chiral strands nor the racemic mixture of the RNA dodecamers with the above sequence

produced diffraction-quality crystals (M. Egli & S. Pitsch, unpublished observations). Therefore, the use of racemic mixtures of shorter DNA and RNA fragments for crystallization experiments is feasible but may have few benefits. The approach has not been tested with longer RNAs, but it is not cost-effective.

Neutron Macromolecular Crystallography

The use of neutron diffraction for analyzing crystal structures of macromolecules has traditionally been hampered by the need for very large crystals and long data collection times. However, several studies of nucleic acid hydration based on neutron diffraction have recently appeared (1, 8, 48). The combination of a spallation neutron source with improvements in instrument design, as proposed for the macromolecular neutron diffractometer (85) to be built at the Oak Ridge National Laboratory in Oak Ridge, Tennessee, is expected to revolutionize neutron macromolecular crystallography. The prospect of neutron diffraction experiments with a resolution of 1.5 Å from crystals $\ll$1 mm^3 in size and lattice repeats in the range of 150 Å is exciting and should greatly benefit structural biology, including analyses of hydration and fine structure of nucleic acid analogs, enzymology, and computational chemistry.

CONCLUDING REMARKS

The search for nucleic acid analogs with improved properties for in vitro and in vivo applications as potential antisense, antigene, aptamer, ribozyme, and, more recently, siRNA agents has been the major driving force for the generation of a large number of chemically modified nucleic acids. A significant subset of these has now been analyzed with structural methods, notably X-ray crystallography. Correlations of the three-dimensional structural data with RNA affinity, nuclease resistance, and, in some cases, cellular uptake have provided guiding principles for the design of modifications with optimized properties for nucleic acid drug discovery. Structures of chemically modified nucleic acids have also yielded fundamental insights into the roles of electrostatics, conformational preorganization, hydration, and stereoelectronic effects, among others, in pairing stability and specificity. Limiting structural studies to native DNA and RNA would not have permitted many of these observations. Nucleic acid analogs also remain the focus of investigations that seek answers to basic questions regarding the origin (nucleic acid etiology) and uniqueness of DNA and RNA. A good example in this context is the recent structure of so-called homo-DNA, which has provided a partial rationalization of nature's preference for pentose to hexose in the genetic system.

SUMMARY POINTS

1. Structural studies of chemically modified nucleic acids and comparisons with the structures of native DNA and RNA molecules have yielded detailed information about the physical and chemical properties of the former, such as the stability of self-pairing and cross-pairing (i.e., RNA affinity), pairing specificity, nuclease resistance, and cellular uptake. The structural data pinpoint several factors that critically affect RNA affinity—a key aspect of modifications in antisense and RNAi applications—such as hydration and stereoelectronic effects involved in conformational preorganization.
2. Structures provide important principles that can guide the design of novel modifications with improved features for applications in high-throughput target validation, drug discovery, and nanotechnology, among others. Investigations of the structures of chemically modified nucleic acids have also led to an improved understanding of

DNA and RNA structure and stability (i.e., the balance of electrostatic and dispersive forces and the roles of water and stereoelectronics).

3. X-ray crystal structures at high resolution offer unique insights into the consequences of chemical modifications for conformation and thermodynamic stability. Particularly in regard to hydration and geometric details, crystallography in combination with computational simulations remains an indispensable tool.
4. Replacement of selected oxygen atoms by sulfur in DNA and RNA has furnished analogs with desirable properties for applications as tools and potentially therapeutics. Thus, PS-DNA exhibits enhanced nuclease resistance and uptake and 4′-thio-RNA shows favorable RNA affinity compared with DNA and RNA, respectively. Structures reveal only minor deviations between geometry and hydration of the modified nucleic acids and those of their natural counterparts.
5. Three-dimensional structures of tetrose (TNA), hexose (homo-DNA and HNA), and PNA have confirmed DNA's unique properties such as the conformational flexibility of the sugar moiety and the relative strengths of self-pairing and cross-pairing with RNA. The structure of homo-DNA revealed a strong inclination between the hexose-phosphate backbone and base-pair planes. The absence of a backbone-base inclination in DNA is the reason for its ability to form duplexes with strands that are either antiparallel or parallel in orientation. Nucleic acid pairing systems with significantly different inclination angles will not pair with each other (e.g., homo-DNA with DNA).
6. Selenoated nucleic acids are emerging as powerful tools for crystallographic phasing. Compared with the well-known derivative preparation with halogenated pyrimidines, selenium can be incorporated at various sites (phosphate, sugar, or base). The resulting analogs are resistant to irradiation with light and intense X-rays and, in most cases, to oxidation.

ACKNOWLEDGMENT

The authors wish to thank the National Institutes of Health (grant R01 GM55237) for continued support.

LITERATURE CITED

1. Arai S, Chatake T, Ohhara T, Kurihara K, Tanaka I, et al. 2005. Complicated water orientations in the minor groove of the B-DNA decamer d(CCATTAATGG)$_2$ observed by neutron diffraction measurements. *Nucleic Acids Res.* 33:3017–24
2. Atwell S, Meggers E, Spraggon G, Schultz PG. 2001. Structure of a copper-mediated base pair in DNA. *J. Am. Chem. Soc.* 123:12364–67
3. **Auffinger P, Westhof E. 2001. Hydrophobic groups stabilize the hydration shell of 2′-O-methylated RNA duplexes. *Angew. Chem. Int. Ed.* 40:4648–50**
4. Berger I, Tereshko V, Ikeda H, Marquez VE, Egli M. 1998. Crystal structures of B-DNA with incorporated 2′-deoxy-2′-fluoro-arabino-furanosyl thymines: implications of conformational preorganization for duplex stability. *Nucleic Acids Res.* 26:2473–80

3. Supports the idea that the higher RNA affinity of 2′-*O*-methyl RNA is the result of a stable water structure around the hydrophobic substituents in the minor groove with long residence times of solvent molecules.

5. Brock CP, Schweizer WB, Dunitz JD. 1991. On the validity of Wallach's rule: on the density and stability of racemic crystals compared with their chiral counterparts. *J. Am. Chem. Soc*. 113:9811–20
6. Chaires JB, Waring MJ, eds. 2001. *Methods in Enzymology: Drug-Nucleic Acid Interactions*, Vol. 340. San Diego: Academic
7. Chan JHP, Lim S, Wong WSF. 2006. Antisense oligonucleotides: from design to therapeutic application. *Clin. Exp. Pharmacol. Phys*. 33:533–40
8. Chatake T, Tanaka I, Umino H, Arai S, Niimura N. 2005. The hydration structure of a Z-DNA hexameric duplex determined by a neutron diffraction technique. *Acta Crystallogr. D* 61:1088–98
9. Crooke ST. 1995. Phosphorothioate oligonucleotides. In *Therapeutic Applications of Oligonucleotides*, ed. ST Crooke, pp. 63–79. Austin, TX: Landes
10. Crooke ST. 1998. Basic principles of antisense therapeutics. In *Antisense Research and Application*, ed. ST Crooke, 131:1–50. Berlin: Springer
11. Dallas A, Vlassov AV. 2006. RNAi: a novel antisense technology and its therapeutic potential. *Med. Sci. Monit.* 12:RA67–74

12. Demonstrated for the first time that all-ANA and all-FANA oligonucleotides paired to RNA are substrates of RNase H.

12. Damha MJ, Wilds CJ, Noronha A, Brukner I, Borkow G, et al. 1998. Hybrids of RNA and arabinonucleic acids (ANA and 2′F-ANA) are substrates of ribonuclease H. *J. Am. Chem. Soc.* 120:12976–77

13. De Napoli L, Iadonisi A, Montesarchio D, Varra M, Piccialli G. 1995. Synthesis of thymidine dimers containing a new internucleosidic amide linkage and their incorporation into oligodeoxyribonucleotides. *Bioorg. Med. Chem. Lett*. 5:1647–52
14. Declercq R, Van Aerschot A, Read RJ, Herdewijn P, Van Meervelt L. 2002. Crystal structure of double helical hexitol nucleic acids. *J. Am. Chem. Soc*. 124:928–33
15. Diop-Frimpong B, Prakash TP, Rajeev KG, Manoharan M, Egli M. 2005. Crystal structure of a DNA duplex with 2′-O-[2-(methoxy)ethyl]-2-thiothymidines: stabilizing contributions of the sulfur-modified nucleotides. *Nucleic Acids Res*. 33:5297–307
16. Doi M, Inoue M, Tomoo K, Ishida T, Ueda Y, et al. 1993. Structural characteristics of enantiomorphic DNA: crystal analysis of racemates of the d(CGCGCG) duplex. *J. Am. Chem. Soc.* 115:10432–33
17. Doudna JA, Lorsch JR. 2005. Ribozyme catalysis: not different, just worse. *Nat. Struct. Mol. Biol*. 12:395–402

18. Initial report of the synthesis of the 2′-SeMe-uridine modification and its use for crystallographic phasing.

18. Du Q, Carasco N, Teplova M, Wilds CJ, Kong X, et al. 2002. Internal derivatization of oligonucleotides with selenium for X-ray crystallography using MAD. *J. Am. Chem. Soc.* 124:24–25

19. Earnshaw J, Gait MJ. 1998. Modified oligoribonucleotides as site-specific probes of RNA structure and function. *Biopolymers* 48:39–55
20. Egholm M, Buchardt O, Christensen L, Behrenst C, Freier SM, et al. 1992. PNA hybridizes to complementary oligonucleotides obeying the Watson-Crick hydrogen-bonding rules. *Nature* 365:566–68
21. Egli M. 1996. Structural aspects of nucleic acid analogs and antisense oligonucleotides. *Angew. Chem. Int. Ed. Engl*. 35:1894–909
22. Egli M. 1998. Conformational preorganization and thermodynamic stability in oligonucleotide duplexes. *Antisense Nucleic Acid Drug Dev*. 8:123–28
23. Egli M. 1998. Towards the structure-based design of nucleic acid therapeutics. In *Advances in Enzyme Regulation*, ed. G Weber, 38:181–203. Oxford, UK: Elsevier
24. Egli M. 2002. DNA-cation interactions: Quo vadis? *Chem. Biol*. 9:277–86
25. Egli M. 2004. Nucleic acid crystallography: current progress. *Curr. Opin. Chem. Biol*. 8:580–91

26. Egli M, Lubini P, Pallan PS. 2007. The long and winding road to the structure of homo-DNA. *Chem. Soc. Rev*. 36:31–45
27. **Egli M, Minasov G, Tereshko V, Pallan PS, Teplova M, et al. 2005. Comprehensive analysis of the RNA affinity, nuclease resistance and crystal structure of ten 2′-O-ribonucleic acid modifications. *Biochemistry* 44:9045–57**
28. **Egli M, Pallan PS, Pattanayek R, Wilds CJ, Lubini P, et al. 2006. Crystal structure of homo-DNA and nature's choice of pentose over hexose in the genetic system. *J. Am. Chem. Soc.* 128:10847–56**
29. Egli M, Portmann S, Usman N. 1996. RNA hydration: a detailed look. *Biochemistry* 35:8489–94
30. Egli M, Tereshko V, Murshudov GN, Sanishvili R, Liu X, et al. 2003. Face-to-face and edge-to-face π-π interactions in a synthetic DNA with a stilbenediether linker. *J. Am. Chem. Soc.* 125:10842–49
31. Ennifar E, Carpentier P, Ferrer JL, Walter P, Dumas P. 2002. X-ray-induced debromination of nucleic acids at the Br K absorption edge and implications for MAD phasing. *Acta Crystallogr. D* 58:1262–68
32. Eschenmoser A. 1999. Chemical etiology of nucleic acid structure. *Science* 284:2118–24
33. Eschenmoser A. 2004. The quest for the chemical roots of life. *Chem. Commun*. pp. 1247–52
34. Eschenmoser A, Dobler M. 1992. Why pentose and not hexose nucleic acids? Part I. *Helv. Chim. Acta* 75:218–59
35. Eschenmoser A, Loewenthal E. 1992. Chemistry of potentially prebiological natural products. *Chem. Soc. Rev*. 21:1–16
36. Fedoroff OY, Salazar M, Reid BR. 1993. Structure of a DNA:RNA hybrid duplex. Why RNase H does not cleave pure RNA. *J. Mol. Biol*. 233:509–23
37. Freier SM, Altmann KH. 1997. The ups and downs of nucleic acid duplex stability: structure-stability studies on chemically-modified DNA:RNA duplexes. *Nucleic Acids Res*. 25:4429–43
38. Gherghe CM, Krahn JM, Weeks KM. 2005. Crystal structures, reactivity and inferred acylation transition states for 2′-amine substituted RNAs. *J. Am. Chem. Soc*. 127:13622–28
39. Griffey RH, Monia BP, Cummins LL, Freier S, Greig MJ, et al. 1996. 2′-*O*-aminopropyl ribonucleotides: a zwitterionic modification that enhances the exonuclease resistance and biological activity of antisense oligonucleotides. *J. Med. Chem.* 39:5100–9
40. **Haeberli P, Berger I, Pallan PS, Egli M. 2005. Syntheses of 4′-thioribonucleosides and thermodynamic stability and crystal structure of RNA oligomers with incorporated 4′-thiocytosine. *Nucleic Acids Res*. 33:3965–75**
41. Hays FA, Teegarden A, Jones ZJ, Harms M, Raup D, et al. 2005. How sequence defines structure: a crystallographic map of DNA structure and conformation. *Proc. Natl. Acad. Sci. USA* 102:7157–62
42. Hendrix DK, Brenner SE, Holbrook SR. 2005. RNA structural motifs: building blocks of a modular biomolecule. *Q. Rev. Biophys*. 38:221–43
43. Hobartner C, Rieder R, Kreutz C, Puffer B, Lang K, et al. 2005. Syntheses of RNAs with up to 100 nucleotides containing site-specific 2′-methylseleno labels for use in X-ray crystallography. *J. Am. Chem. Soc.* 127:12035–45
44. Hoshika S, Minakawa N, Matsuda A. 2004. Synthesis and physical and physiological properties of 4′-thioRNA: application to post-modification of RNA aptamer toward NF-κB. *Nucleic Acids Res*. 32:3815–25

27. Investigates the role of RNA 2′-O-substituents in the modulation of RNA affinity and nuclease resistance.

28. A structural rationalization of why fully hydroxylated hexopyranose-based nucleic acid systems [e.g., (4′→6′)-linked oligo-β-D-glucose nucleic acid] are unable to pair.

40. Reports the chemical synthesis and favorable RNA affinity of RNA with the 4′-oxygen of ribose replaced by sulfur.

45. Hud NV, Polak M. 2001. DNA-cation interactions: The major and minor grooves are flexible ionophores. *Curr. Opin. Struct. Biol.* 11:293–301
46. Hunziker J, Roth HJ, Böhringer M, Giger A, Diedrichsen U, et al. 1993. Why pentose and not hexose nucleic acids? Part III. *Helv. Chim. Acta* 76:259–52
47. Inoue N, Minakawa N, Matsuda A. 2006. Synthesis and properties of 4′-thioDNA: unexpected RNA-like behavior of 4′-thioDNA. *Nucleic Acids Res.* 34:3476–83
47a. Juan ECM, Kondo J, Kurihara T, Ito T, Ueno Y, et al. 2007. Crystal structures of DNA:DNA and DNA:RNA duplexes containing 5-(N-aminohexyl)carbamoyl-modified uracils reveal the basis for properties as antigene and antisense molecules. *Nucleic Acids Res.* 35:In press
47b. Komeda S, Moulaei T, Woods KK, Chikuma M, Farrell NP, Williams LD. 2006. A third mode of DNA binding: phosphate clamps by a polynuclear platinum complex. *J. Am. Chem. Soc.* 128:16092–103
48. Langan P, Li X, Hanson BL, Coates L, Mustyakimov M. 2006. Synthesis, capillary crystallization and preliminary joint X-ray and neutron crystallographic study of Z-DNA without polyamine at low pH. *Acta Crystallogr. F* 62:453–56
49. Lewis FD, Liu X, Wu Y, Miller S, Wasielewski MR, et al. 1999. Structure and photoinduced electron transfer in exceptionally stable synthetic DNA hairpins with stilbenediether linkers. *J. Am. Chem. Soc.* 121:9905–6
50. Lewis FD, Letsinger RL, Wasielewski MR. 2001. Dynamics of photoinduced charge transfer and hole transport in synthetic DNA hairpins. *Acc. Chem. Res.* 34:159–70
51. Li F, Sarkhel S, Wilds CJ, Wawrzak Z, Prakash TP, et al. 2006. 2′-Fluoroarabino- and arabinonucleic acid show different conformations, resulting in deviating RNA affinities and processing of their heteroduplexes with RNA by RNase H. *Biochemistry* 45:4141–52
52. Lima WF, Crooke ST. 1997. Binding affinity and specificity of *Escherichia coli* RNase H1: impact on the kinetics of catalysis of antisense oligonucleotide-RNA hybrids. *Biochemistry* 36:390–98
53. Lubini P, Zürcher W, Egli M. 1994. Crystal structure of an oligodeoxynucleotide duplex containing 2′-O-methylated adenosines. *Chem. Biol.* 1:39–45
54. Deleted in proof
55. Maier T, Przylas I, Strater N, Herdewijn P, Saenger W. 2005. Reinforced HNA backbone hydration in the crystal structure of a decameric HNA/RNA hybrid. *J. Am. Chem. Soc.* 127:2937–43
56. Manoharan M. 1999. 2′-Carbohydrate modifications in antisense oligonucleotide therapy: importance of conformation, configuration and conjugation. *Biochim. Biophys. Acta* 1489:117–30
57. Manoharan M. 2004. RNA interference and chemically modified small interfering RNAs. *Curr. Opin. Chem. Biol.* 8:570–79
58. Menchise V, De Simone G, Tedeschi T, Corradini R, Sforza S, et al. 2003. Insights into peptide nucleic acid (PNA) structural features: the crystal structure of a D-lysine-based chiral PNA-DNA duplex. *Proc. Natl. Acad. Sci. USA* 100:12021–26
59. Minasov G, Matulic-Adamic J, Wilds CJ, Haeberli P, Usman N, et al. 2000. Crystal structure of an RNA duplex containing phenyl-ribonucleotides, hydrophobic isosteres of the natural pyrimidines. *RNA* 6:1516–28
60. Minasov G, Teplova M, Nielsen P, Wengel J, Egli M. 2000. Structural basis of cleavage by RNase H of hybrids of arabinonucleic acids and RNA. *Biochemistry* 39:3525–32
61. Mooers BH, Logue JS, Berglund JA. 2005. The structural basis of myotonic dystrophy from the crystal structure of CUG repeats. *Proc. Natl. Acad. Sci. USA* 102:16626–31

62. Morales JC, Kool ET. 1998. Efficient replication between non-hydrogen-bonded nucleoside shape analogs. *Nat. Struct. Biol.* 5:950–54
63. Moroder H, Kreutz C, Lang K, Serganov A, Micura R. 2006. Synthesis, oxidation behavior, crystallization and structure of 2′-methylseleno guanosine containing RNAs. *J. Am. Chem. Soc.* 128:9909–18
64. Moulaei T, Maehigashi T, Lountos GT, Komeda S, Watkins D, et al. 2005. Structure of B-DNA with cations tethered in the major groove. *Biochemistry* 44:7458–68
65. Nakamura H, Oda Y, Iwai S, Inoue H, Ohtsuka E, et al. 1991. How does RNase H recognize a DNA:RNA hybrid? *Proc. Natl. Acad. Sci. USA* 88:11535–39
66. Nielsen PE, Egholm M, Berg RH, Buchardt O. 1991. Sequence-selective recognition of DNA by strand displacement with a thymine-substituted polyamide. *Science* 254:1497–500
67. Noller HF. 2005. RNA structure: reading the ribosome. *Science* 309:1508–14
68. Nowotny M, Gaidamakov SA, Crouch RJ, Yang W. 2005. Crystal structures of RNase H bound to an RNA/DNA hybrid: substrate specificity and metal-dependent catalysis. *Cell* 121:1005–16
69. Ogawa AK, Wu Y, McMinn DL, Liu J, Schultz PG, et al. 2000. Efforts toward the expansion of the genetic alphabet: information storage and replication with unnatural hydrophobic base pairs. *J. Am. Chem. Soc.* 122:3274–87
70. Pallan PS, Wilds CJ, Wawrzak Z, Krishnamurthy R, Eschenmoser A, et al. 2003. Why does TNA bind more strongly to RNA than to DNA? An answer from X-ray analysis. *Angew. Chem. Intl. Ed. Engl.* 42:5893–95
71. Pallan PS, von Matt P, Wilds CJ, Altmann KH, Egli M. 2006. RNA-binding affinities and crystal structure of oligonucleotides containing five-atom amide-based backbone structures. *Biochemistry* 45:8048–57
72. Park H, Zhang K, Ren Y, Nadji S, Sinha N, et al. 2002. Crystal structure of a DNA decamer containing a *cis-syn* thymine dimer. *Proc. Natl. Acad. Sci. USA* 99:15965–70
73. Pattanayek R, Sethaphong L, Pan C, Prhavc M, Prakash TP, et al. 2004. Structural rationalization of a large difference in RNA affinity despite a small difference in chemistry between two 2′-*O*-modified nucleic acid analogs. *J. Am. Chem. Soc.* 126:15006–7
74. Pavletich NP, Pabo CO. 1991. Zinc finger-DNA recognition: crystal structure of a Zif268-DNA complex at 2.1 Å. *Science* 252:809–17
75. Petersson B, Nielsen BB, Rasmussen H, Larsen IK, Gajhede M, et al. 2005. Crystal structure of a partly self-complementary peptide nucleic acid (PNA) oligomer showing a duplex-triplex network. *J. Am. Chem. Soc.* 127:1424–30
76. Piccirilli JA, Krauch T, Moroney SE, Benner SA. 1990. Enzymatic incorporation of a new base pair into DNA and RNA extends the genetic alphabet. *Nature* 343:33–37
77. Prakash TP, Manoharan M, Fraser AS, Kawasaki AM, Lesnik E, et al. 2002. 2′-O-[2-(methylthio)ethyl]-modified oligonucleotide: an analog of 2′-O-[2-(methoxy)ethyl]-modified oligonucleotide with improved protein binding properties and high binding affinity to target RNA. *Biochemistry* 41:11642–48
78. Prakash TP, Püeschl A, Lesnik E, Mohan V, Tereshko V, et al. 2004. 2′-O-[2-(guanidinium)ethyl]-modified oligonucleotides: stabilizing effect on duplex and triplex structures. *Org. Lett.* 6:1971–74
79. Prhavc M, Prakash TP, Minasov G, Egli M, Manoharan M. 2003. 2′-O-[2-[2-(N,N-dimethylamino)ethoxy]ethyl] modified antisense oligonucleotides: symbiosis of charge interaction factors and stereoelectronic effects. *Org. Lett.* 5:2017–20
80. Rasmussen H, Kastrup JS, Nielsen JN, Nielsen JM, Nielsen PE. 1997. Crystal structure of a peptide nucleic acid (PNA) duplex at 1.7 Å resolution. *Nat. Struct. Biol.* 4:98–101

81. Rasmussen H, Liljefors T, Petersen B, Nielsen PE, Kastrup JS. 2004. The influence of a chiral amino acid on the helical handedness of PNA in solution and in crystals. *J. Biomol. Struct. Dyn*. 21:1–8
82. Rich A. 2003. The double helix: a tale of two puckers. *Nat. Struct. Biol*. 10:247–49
83. Rypniewski W, Vallazza M, Perbandt M, Klussmann S, DeLucas LJ, et al. 2006. The first crystal structure of an RNA racemate. *Acta Crystallogr. D* 62:659–64
84. Schöning KU, Scholz P, Guntha S, Wu X, Krishnamurthy R, et al. 2000. Chemical etiology of nucleic acid structure: the α-threofuranosyl-(3′→2′) oligonucleotide system. *Science* 290:1347–51
85. Schultz AJ, Thiyagarajan P, Hodges JP, Rehm C, Myles DAA, et al. 2005. Conceptual design of a macromolecular neutron diffractometer (MaNDi) for the SNS. *J. Appl. Crystallogr.* 38:964–74
86. Serganov A, Keiper S, Malinina L, Tereshko V, Skripkin E, et al. 2005. Structural basis for Diels-Alder ribozyme-catalyzed carbon-carbon bond formation. *Nat. Struct. Mol. Biol.* 12:218–24
87. Stellwagen N, Mohanty U, eds. 2004. *Curvature and Deformation of Nucleic Acids: Recent Advances, New Paradigms*. ACS Symp. Ser., Vol. 884. Washington, DC: Am. Chem. Soc.
88. Subirana JA. 2005. The structures of DNA. *Mem. Real Acad. Cienc. Artes Barc.* Vol. LXII, No. 1, pp. 3–30
89. Sung CH, Lowenhaupt K, Rich A, Kim YG, Kim KK. 2005. Crystal structure of a junction between B-DNA and Z-DNA reveals two extruded bases. *Nature* 437:1183–86
90. Teplova M, Minasov G, Tereshko V, Inamati G, Cook PD, et al. 1999. Crystal structure and improved antisense properties of 2′-O-(2-methoxyethyl)-RNA. *Nat. Struct. Biol.* 6:535–39
91. Teplova M, Wallace ST, Minasov G, Tereshko V, Symons A, et al. 1999. Structural origins of the exonuclease resistance of a zwitterionic RNA. *Proc. Natl. Acad. Sci. USA* 96:14240–45
92. Teplova M, Wilds CJ, Wawrzak Z, Tereshko V, Du Q, et al. 2002. Covalent incorporation of selenium into oligonucleotides for X-ray crystal structure determination via MAD: proof of principle. *Biochimie* 84:849–58
93. Tereshko V, Gryaznov S, Egli M. 1998. Consequences of replacing the DNA 3′-oxygen by an amino group: high-resolution crystal structure of a fully modified N3′→P5′ phosphoramidate DNA dodecamer duplex. *J. Am. Chem. Soc*. 120:269–83
94. Tereshko V, Portmann S, Tay E, Martin P, Natt F, et al. 1998. Structure and stability of DNA duplexes with incorporated 2′-O-modified RNA analogues. *Biochemistry* 37:10626–34
95. Tereshko V, Wilds CJ, Minasov G, Prakash TP, Maier MA, et al. 2001. Detection of alkali metal ions in DNA crystals using state-of-the-art X-ray diffraction experiments. *Nucleic Acids Res*. 29:1208–15
96. Thore S, Leibundgut M, Ban N. 2006. Structure of the eukaryotic thiamine pyrophosphate riboswitch with its regulatory ligand. *Science* 312:1208–11
97. Vallazza M, Perban M, Klussman S, Rypniewski W, Einspahr HM, et al. 2004. First look at RNA in L-configuration. *Acta Crystallogr. D* 60:1–7
98. Verma S, Eckstein F. 1998. Modified oligonucleotides: synthesis and strategy for users. *Annu. Rev. Biochem*. 67:99–134
99. Walder RT, Walder JA. 1988. Role of RNase H in hybrid-arrested translation by antisense oligonucleotides. *Proc. Natl. Acad. Sci. USA* 85:5011–15
100. Wilds CJ, Damha MJ. 2000. 2′-Deoxy-2′-fluoro-β-D-arabinonucleosides and oligonucleotides (2′F-ANA): synthesis and physicochemical studies. *Nucleic Acids Res*. 28:3625–35

86. Describes the first crystal structure of a novel RNA folding-motif determined with a 2′-SeMe-uridine derivative.

101. Wilds CJ, Maier MA, Tereshko V, Manoharan M, Egli M. 2002. Direct observation of a cytosine analogue that forms five hydrogen bonds to guanosine: guanidino G-clamp. *Angew. Chem. Int. Ed.* 114:123–25

102. Wilds CJ, Pattanayek R, Pan C, Wawrzak Z, Egli M. 2002. Selenium-assisted nucleic acid crystallography: use of DNA phosphoroselenoates for MAD phasing. *J. Am. Chem. Soc.* 124:14910–16

103. Wilds CJ, Wawrzak Z, Krishnamurthy R, Eschenmoser A, Egli M. 2002. DNA duplex containing (L)-α-threofuranosyl (3′-2′) nucleosides (TNA): A simple four carbon sugar is easily accommodated into the backbone of DNA. *J. Am. Chem. Soc.* 124:13716–21

104. Xia J, Noronha A, Toudjarska I, Li F, Akinc A, et al. 2006. siRNAs with a ribo-difluorotoluyl nucleotide: structure, RISC-mediated recognition, and silencing. *ACS Chem. Biol.* 1:176–83

102. Proof of principle study of the use of phosphoroselenoate nucleic acids for crystallographic phasing.